

Geometric Transformation Algorithm for Acetabular Cup Orientation: Converting 2D Radiographic Projections to 3D Spatial Positioning

GÖKMEN AKTAS^{1*}, LUKAS HENSLER², SABINE DIPPEL², PIA HEINS², JORGE MAYOR¹, JAN-DIERK CLAUSEN¹, EMMANOUIL LIODAKIS¹, STEPHAN SEHMISCH¹ and TAREK OMAR PACHA^{1*}

¹Department of Trauma Surgery, Hannover Medical School, Hannover, Germany;

²University of Applied Sciences and Arts, Department of Electrical Engineering and Information Technology, Hannover, Germany

Abstract

Background/Aim: Hip replacement is one of the most common and successful surgeries of our time. However, with increasing numbers of total hip arthroplasties, postoperative complications due to inadequate cup positioning are rising. Accurate measurement of acetabular cup inclination and anteversion is critical for optimal outcomes. While various measurement systems exist, they often require additional hardware, specialized training, or lack integration across the care continuum. This study aims to develop and validate software for automated measurement of acetabular cup positioning, comparing its performance to standard CAD measurements.

Materials and Methods: The geometric basis for analyzing the acetabular cup is that a hemisphere in 2D projection forms an ellipse, described by a conic section equation. We developed a Python-based software utilizing computer vision techniques for edge detection and ellipse fitting to determine anteversion and inclination from standard radiographs. The software was trained and validated using X-ray images of a pelvic phantom with a conventional acetabular cup (Allofit, Zimmer Biomet) at various predefined angles. CAD software (MediCAD) served as the validation standard. The intraclass correlation coefficient (ICC) quantified agreement between methods.

Results: A total of 140 AP X-ray images were analyzed. Inclination averaged $50.69^{\circ} \pm 15.86^{\circ}$ with our software versus $49.40^{\circ} \pm 15.24^{\circ}$ with CAD. Anteversion averaged $14.36^{\circ} \pm 9.08^{\circ}$ versus $14.75^{\circ} \pm 8.88^{\circ}$ with CAD. The ICC was 0.994 for inclination and 0.992 for anteversion (both $p < 0.001$), demonstrating excellent agreement.

continued

*These Authors contributed equally to the present study.



Gökmen Aktas, Carl-Neuberg St. 1, Hannover 30625, Lower Saxony, Germany. Tel: +49 1708141024, e-mail: aktas.goekmen@mh-hannover.de

Received January 20, 2026 | Revised February 15, 2026 | Accepted March 23, 2026



This is an open access article under the terms of the Creative Commons Attribution License, which permits use, distribution and reproduction in any medium, provided the original work is properly cited.

©2026 The Author(s). Anticancer Research is published by the International Institute of Anticancer Research.

Conclusion: Our computer-assisted measurement technique demonstrates excellent concordance with standard methodologies while offering workflow advantages. These results provide a foundation for implementation within computer vision models for automated spatial positioning recognition. Future development will focus on enhancing automation, validating across diverse populations and implant designs, and comparing with 3D computed tomography (CT) measurements.

Keywords: Artificial intelligence, arthroplasty, hip, surgery, traumatology, computer vision.

Introduction

Total hip arthroplasty (THA) is charmingly referred to as the operation of the century within the orthopedic community (1). In the 1960s, hip arthroplasty, “a new operation,” revolutionized the management of patients suffering from hip osteoarthritis (2). In the USA, between 2006 and 2014, there was a 69.50% increase in patients receiving a primary hip prosthesis (3). Due to demographic changes and the aging population, this trend is expected to continue, leading to not only more primary implantations but also an inevitable rise in complication rates (3). However, it is also observed that the number of revision surgeries in hip endoprosthetics is increasing as well. There was a 28.50% increase in revision surgeries between 2006 and 2014 (3).

With the increasing number of both primary and revision total hip replacements, there is a critical need to address factors that contribute to complications, particularly dislocation, and resulting revision surgeries (4). Postoperative complications after THA include heterotopic ossifications, periprosthetic fractures, infections, material wear, impingement, and acetabular dislocations (4). Proper positioning of the acetabular cup is one such crucial factor, directly impacting patient outcomes, such as impingement and accelerated wear (5, 6).

The positioning of the acetabular cup during the implantation of a total hip arthroplasty is essential to ensure optimal surgical outcomes and to prevent complications (7). The key parameters for cup positioning are inclination and anteversion relative to the patient’s hip

(7-9). While these key orientation factors can generally be assessed with conventional X-rays, there is criticism regarding the applicability of the methodology, as it is influenced by multiple factors (10-12). Regarding the orientation of the acetabular cup in space and in relation to anatomical anchor points, various modern procedures are proposed in the literature (13). These range from the purely manual use of a goniometer to the use of CT and invasive navigation methods; however, the multitude of proposed procedures and the variability in surgeon experience suggest that no universally accepted standard has been established in clinical practice (14-18).

Computer vision (CV), a well-established subset of artificial intelligence (AI), has demonstrated remarkable capabilities in medical image analysis. With powerful open-access frameworks like YOLO (you only look once) and others widely available, automated detection and measurement of anatomical structures and implants has become increasingly accessible, improving consistency and reducing analysis time (9, 19-22). While CV technology itself is mature and readily implementable, its specific application to acetabular cup positioning analysis represents an opportunity for innovation.

In this study, we propose an algorithm that leverages existing CV frameworks to automatically detect the acetabular cup in X-ray images. However, the critical advancement lies not in the CV-based detection itself, but in the subsequent mathematical transformation that converts the two-dimensional elliptical projection in standard X-rays into an accurate three-dimensional position determination of the cup, specifically quantifying its anteversion and inclination angles. This

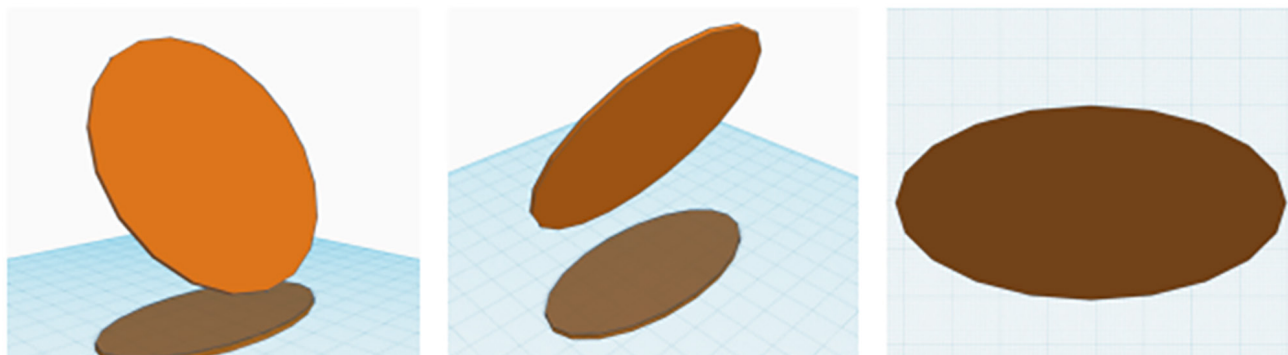


Figure 1. Graphical illustration of a circle in three-dimensional space with elliptical shadow projections onto a horizontal plane.

work represents an essential first step toward clinical implementation by validating our mathematical and computational framework against current standard CAD measurements, establishing a foundation for a more efficient and accessible tool in hip arthroplasty assessment.

Materials and Methods

Overview of the approach. The approach to software-assisted geometry analysis in hip arthroplasty builds on a comprehensive framework comprising four interconnected components. The foundation is a mathematical model based on geometric principles of elliptical projections, which informs the computer vision algorithms for image processing and feature detection. These components are integrated into a user-friendly software with a graphical interface, and the entire system is validated through comparison with established CAD measurements using standardized phantom radiographs. Figure 1 provides an overview of the complete workflow from radiograph acquisition to final measurement output.

Geometrical and mathematical background. The geometrical basis for the analysis of the acetabular cup relies on the principle that a hemisphere in a 2D projection image forms an ellipse. This fundamental relationship allows inference of the position of the “hemisphere” in three-dimensional space from its elliptical projection, using appropriate mathematical

algorithms (Figure 1). Accordingly, to determine the inclination and anteversion of a hip cup in radiographic images, the elliptical projection of its circular boundary onto the image plane can be utilized.

Mathematical framework and parameter definition. To determine the inclination and anteversion of a hip implant within radiographic images, the projection of its circular edge onto the image plane can be modeled as an ellipse (Figure 1). The shape of this ellipse is described by the general form of the conic section equation formula:

$$Ax^2 + By^2 + Cxy + Dx + Ey + F = 0$$

The coefficients A, B, and C define the ellipse’s shape and orientation, with A and B representing quadratic scaling in x and y directions, and C encoding rotation. The linear terms D and E control translation, while F provides normalization. These six parameters are uniquely determined from five points on the ellipse contour or by defining the major axis endpoints. The conic section forms an ellipse when $C^2 - 4AB < 0$, and a parabola when $C^2 - 4AB = 0$.

The transformation from 2D projection to 3D spatial positioning relies on two key geometric relationships (Figure 2D, E). First, the inclination angle α derives from the ellipse rotation in the image plane through $\alpha = 0.5 \times \arctan(C/(A-B))$, where the factor 0.5 accounts for angle doubling in the conic equation. Second, the anteversion angle γ follows from the principle that a tilted circular cup projects as an ellipse, with the axis ratio encoding the tilt magnitude.

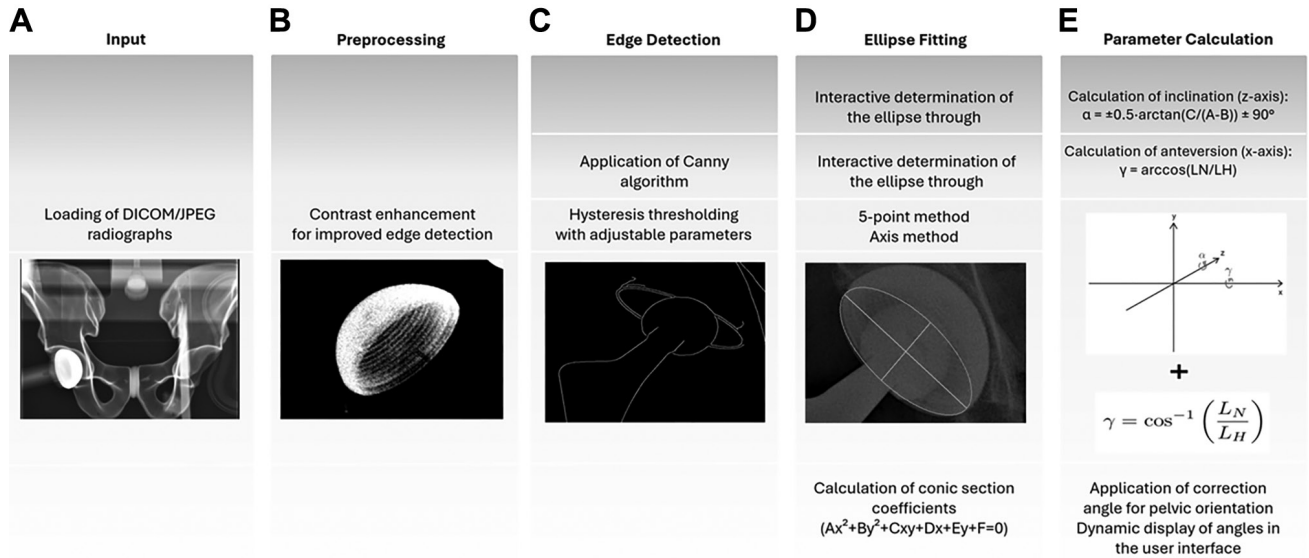


Figure 2. Overview of the software-assisted workflow for acetabular cup position measurement, showing the progression from radiograph acquisition through image processing, ellipse detection, and angle calculation. M: Manually performed; SA: semi-automatically performed; A: automatically performed.

Inclination/Anteversion. The three-dimensional cup projects an ellipse in two-dimensional space (Figure 1). The inclination around the z-axis is calculated using the formula $\alpha = 0.5 \cdot \arctan(C/(A-B))$ derived from the conic section coefficients (Figure 2E). This represents the ellipse rotation relative to the image axes, providing the cup's medial-lateral tilt. The anteversion along the x-axis is determined through $\gamma = \arccos(L_N/L_H)$, where L_H and L_N represent the major and minor axis lengths respectively. These lengths are computed from the conic coefficients as:

$$L_H, L_N = \sqrt{[(AE^2 + BD^2 - 4CDE - 4ABF) / (4C^2 - AB \mp \sqrt{((A-B)^2 + C^2) - (A+B)})]}$$

This relationship exploits the geometric principle that a circular cup tilted by angle γ projects as an ellipse with axis ratio $L_N/L_H = \cos(\gamma)$. The major axis L_H corresponds to the true cup diameter, while L_N represents its foreshortened projection.

A correction angle θ is applied to reference measurements to pelvic anatomy rather than image coordinates, yielding the final inclination $\alpha_{final} = \alpha + \theta$. Unlike traditional methods, this approach does not require referencing a horizontal line at the symphysis or the ischial tuberosities for basic

measurements, though this anatomical reference can be incorporated if desired.

Implementation. Ellipse detection and fitting. Currently, the workflow is implemented as a semi-automated process (Figure 2). After manually loading an image, preprocessing and edge detection can be executed by the software using several Python libraries and filters (Figure 2A-C). The user can then either mark five points along the cup boundary or define the major and minor axes of the ellipse (Figure 2D). Based on these inputs, the system solves the conic section equation to determine the parameters A through F that best fit the selected points or axes. Both direct algebraic fitting and least-squares optimization approaches have been implemented to accommodate different user inputs and varying image qualities. While the primary focus of this paper is on the mathematical transformation algorithm that converts the 2D elliptical projection into the 3D cup orientation, we are concurrently developing a fully automated detection system. In this parallel work, the Random Sample Consensus (RANSAC) algorithm identifies candidate ellipses from the edge points and selects the most probable cup boundary based on geometric

constraints typical of acetabular cups. It should be noted that RANSAC itself is not a computer vision technique but rather a robust mathematical fitting algorithm, serving as an important bridge between our mathematical transformation and its future integration into a comprehensive computer vision model (Figure 2E). This approach currently achieves approximately 80% successful automatic detection in phantom images and will be integrated with the mathematical transformation algorithm described here in future iterations. Figure 2 illustrates the software-assisted workflow with the various manual or (semi-)automated steps leading up to the mathematical transformation of the 3D cup orientation. In this context, “manual” refers to loading an image or drawing the ellipse, whereas “semi-automated” is defined as the application of the procedure through a single user command, upon which the algorithm is executed automatically.

Software development and implementation. For analysis of X-ray images using the mathematical principles described above, a program in Python 3.9.19 (Newark, DE, USA) was developed that integrates a user interface with comprehensive image processing capabilities. The development was conducted on a personal computer running Windows 10 Enterprise (Microsoft, Redmond, WA, USA). Through the implementation of various Python classes, a standalone software application was created capable of importing and analyzing both DICOM and JPEG files, as shown in Figure 3.

Software architecture and libraries. The software was developed with Python 3.9.19 using several specialized libraries for different functional aspects. For image processing, scikit-image (0.19.2) was utilized, while NumPy (1.22.3) provided the necessary tools for numerical operations and array manipulations. Visualization and plotting were handled with Matplotlib (3.5.1), and the graphical user interface was built using Tkinter (Figure 4). Medical image file handling was managed through pydicom (2.3.0), and PyInstaller (5.0.1) was employed to create a standalone executable application.

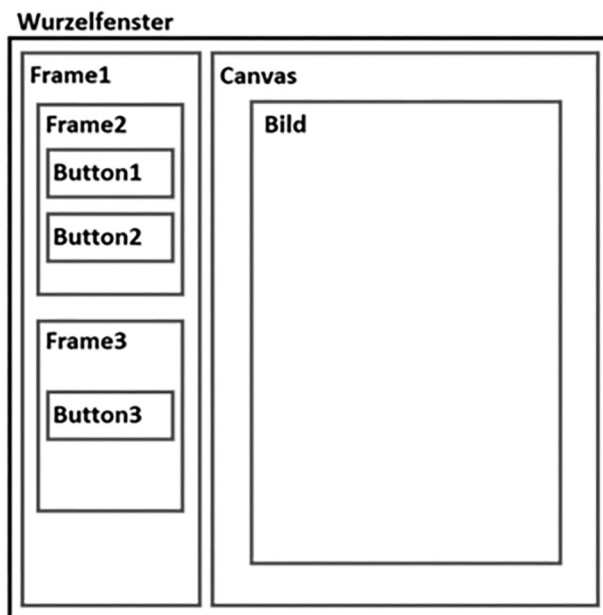


Figure 3. User interface of the software created in Python within the Tkinter package.

Validation methodology. Hip-Phantom. To obtain highly controlled radiographs for system validation, a specialized pelvic phantom was developed consisting of a Full Male Pelvis (Absolute™ 4th Generation 17 PCF Solid Foam Core, Large, Sawbone Europe, Malmö, Sweden) fitted with a conventional acetabular cup (Allofit, Alloclassic, Zimmer Biomet, Zug, Switzerland). The cup was attached to the Sawbone pelvis using a plexiglass fixture, and the mounting arm allowed specific positioning of the cup at predetermined inclination and anteversion angles (Figure 4).

This phantom design enabled the creation of X-ray images depicting various cup orientations under controlled conditions. The plexiglass material was chosen to minimize interference with the images, optimizing the model to contain as few confounding factors as possible. The setup allowed for the recording of numerous X-ray images at different angles, including extreme positions. In addition to anteversion and inclination adjustments in 0.5° increments, the entire pelvis could be tilted both horizontally and vertically to simulate different radiographic perspectives.

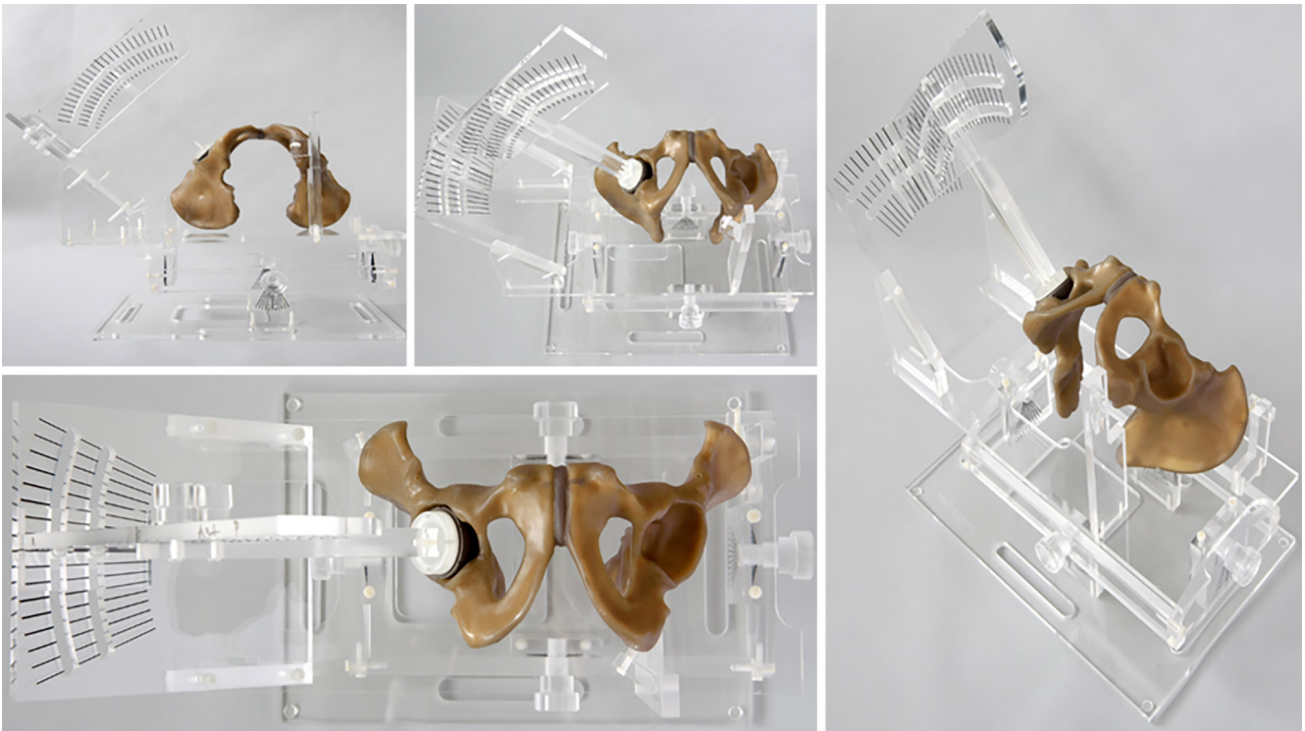


Figure 4. Original image of the pelvic phantom in the Plexiglas device in various planes.

Measurements. After X-ray images with different angle settings were captured, they were exported in DICOM format and loaded into the software. As the next step, we placed 5 points along the cup boundary from which RANSAC automatically completed the ellipse detection, or alternatively, users could draw the cup axis directly (Figure 5). Notably, this approach eliminated the need for a reference line (required in traditional CAD measurements) for calculating inclination and anteversion and did not require sphere-based scaling.

For validation, the same X-ray images were independently analyzed by an experienced orthopedic surgeon using MediCAD (MediCAD Hectec GmbH, Germany, Altdorf Version 3.0.29.21822), a commercial software for planning and analyzing orthopedic surgeries. MediCAD offers a tool to determine hip implant inclination in postoperative mode, accessible through the manual planning function in the postoperative section. After importing and scaling an image, the user must define

the implant side relative to the hip and draw a reference line to access the “Inclination/Anteversion” feature. The two major axes are positioned manually to determine inclination, followed by ellipse adjustment for anteversion measurement (Figure 6).

The orthopedic surgeon scaled each image in MediCAD using a reference sphere or the implanted hip cup when available. A reference line was drawn at both ischial tuberosities, followed by drawing the hip cup axis and adjusting the ellipse to the appropriate size. The resulting measurements of inclination (CAD-I) and anteversion (CAD-A) were then statistically compared with the software’s measurements (S-I and S-A).

Experimental protocol. For comprehensive validation, a dataset comprising 140 anteroposterior (AP) radiographs of the phantom was acquired, featuring the acetabular cup positioned across diverse orientations. The cup placement encompassed a broad angular spectrum, with inclination

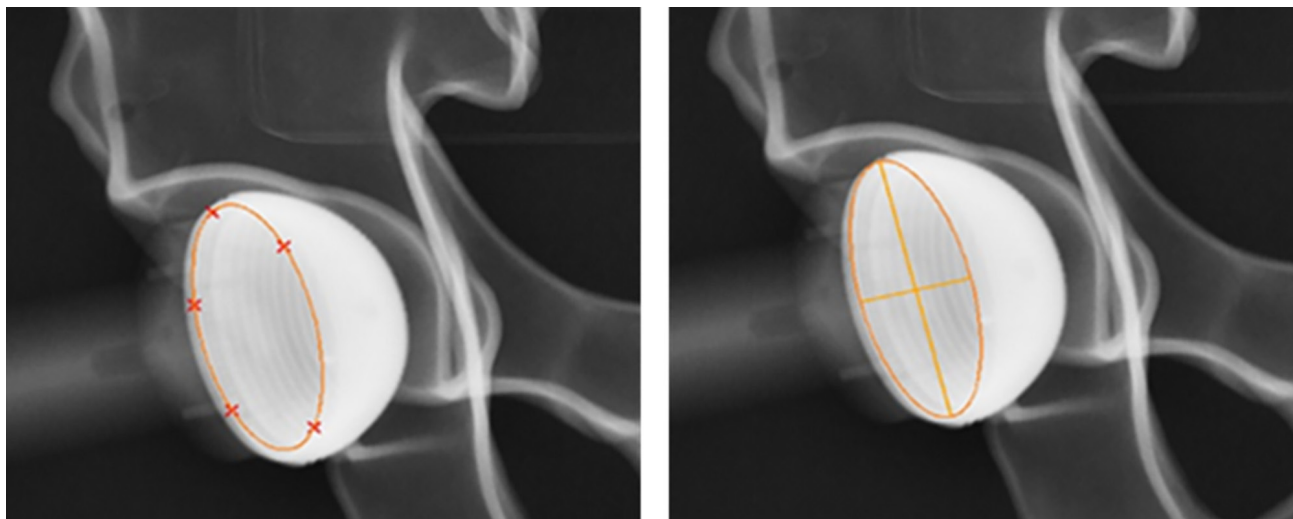


Figure 5. Interface of the developed program with five points or axis determining the ellipse.

values ranging from 15° to 88° and anteversion measurements spanning 1° to 35° .

A standardized analytical protocol was implemented for each radiographic image: initially, the image underwent analysis via our software utilizing semi-automated ellipse fitting with RANSAC algorithm implementation; subsequently, independent assessment of the identical image was conducted by an experienced orthopedic surgeon employing the MediCAD software; tertiary, quantitative measurements of both inclination and anteversion angles were documented from both methodological approaches; and finally, statistical analysis was performed to evaluate comparative outcomes. This experimental methodology facilitated direct comparative assessment between our mathematical transformation algorithm and the contemporary standard computer-aided design approach under controlled conditions with predetermined geometrical parameters.

Statistical analysis. The statistical analysis was performed using SPSS (version 28.0, IBM Corp., Armonk, NY, USA) on a Windows 10 Professional system. For each measurement method (AI and CAD), descriptive statistics including minimum, maximum, mean, standard deviation, and variance calculation were conducted.

To assess normality of distribution, both Kolmogorov-Smirnov and Shapiro-Wilk tests were performed. Inter-rater reliability between the software and CAD measurements was quantified using the intraclass correlation coefficient (ICC), applying a two-way mixed model with absolute agreement. Following established guidelines, reliability was considered poor with ICC <0.5 and good to excellent with ICC $>0.8-0.9$. The significance level was set at $\alpha=0.05$ (two-tailed) for ICC calculations (23, 24).

Ethical approval. This research was conducted in accordance with the Declaration of Helsinki and received approval from the local Hannover Medical School Research Ethics Committee with no concerns raised.

Results

In this study, a total of 140 anterior-posterior radiographic images of a pelvic phantom were analyzed to validate the measurements of the software-assisted measurement against CAD measurement techniques in the first step. The inclination measurements showed high consistency between the two methods: The software yielded a mean inclination of 50.69° [standard deviation (SD)=15.86],

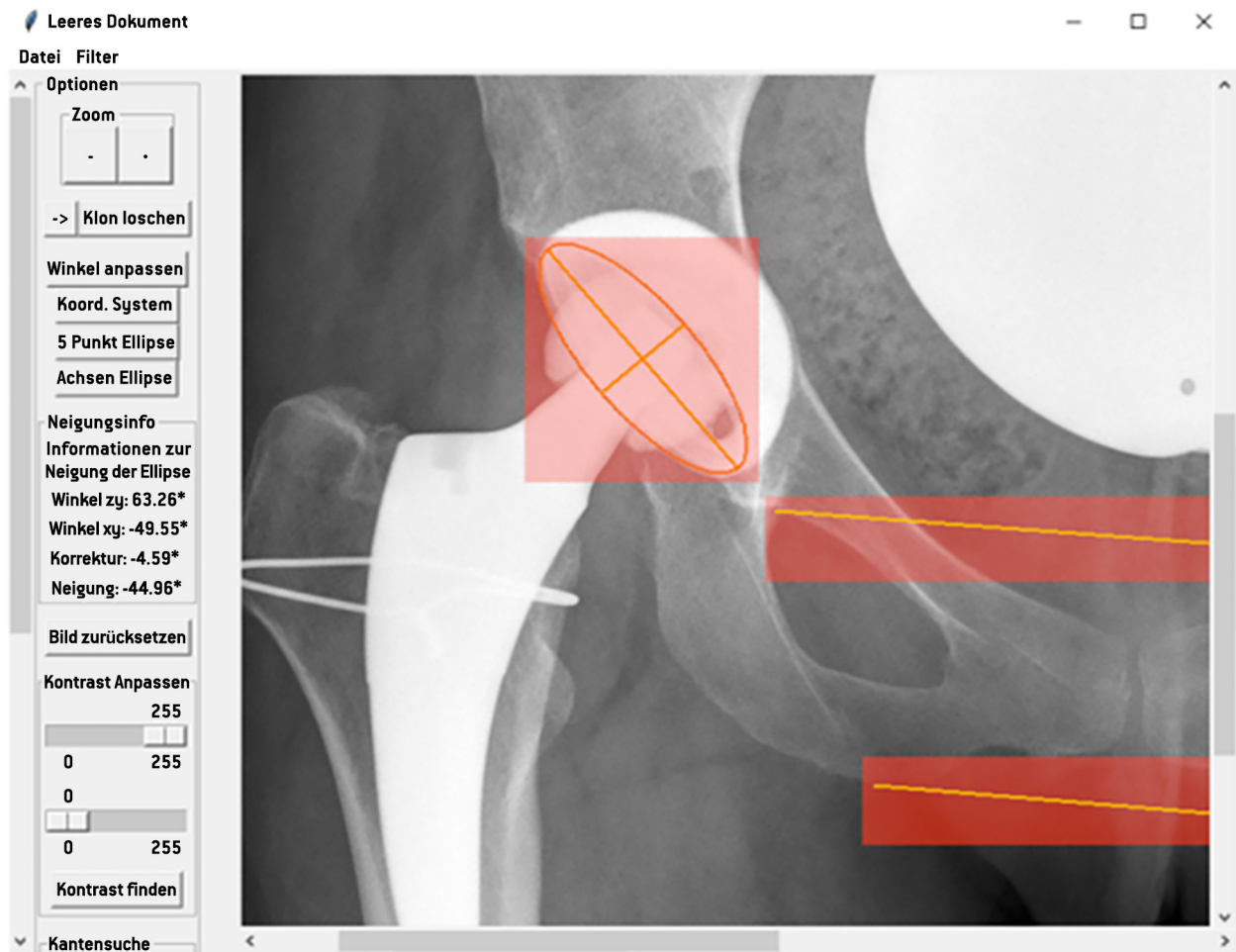


Figure 6. Illustration of the combined Python classes for automated acetabulum detection and ellipse creation.

compared to 49.40° ($SD=15.24$) for the CAD measurement (Table I). The measurement range was between 15° and 88° for the software method and between 15° and 85° for CAD measurements (Table I). The lowest measured inclination was 15° for both methods, while the highest inclination was 88° for the software and 85° for the CAD measurement (Table I).

The anteversion measurements showed similarly high precision. The software calculated a mean of 14.36° ($SD=9.08$), which was close to the CAD mean of 14.75° ($SD=8.88$). The measurement range for anteversion extended from 1° to 35° for the software and from 1° to 34° for the CAD measurement. The lowest measured

anteversion was 1° for both methods, while the highest anteversion was 35° for the software and 34° for the CAD measurement (Table I).

Normality tests (Kolmogorov-Smirnov and Shapiro-Wilk) showed different results for the inclination measurements and the anteversion measurements. For the inclination measurements, both methods yielded a normal distribution (AI-I: $p=0.200$, $p=0.513$; CAD-I: $p=0.200$, $p=0.670$) (Table I). In contrast, the anteversion measurements showed a more complex distribution pattern, with the software method not showing a normal distribution (AI-A: $p=0.029$, $p=0.001$). The CAD anteversion measurements showed a borderline distribution, as the null hypothesis of normality could be

Table I. Descriptive statistics, normality testing, and inter-rater reliability analysis comparing software-based and CAD-based measurements of acetabular cup inclination and anteversion in 140 anteroposterior pelvic phantom radiographs.

Statistics	S-I (Inclination)	CAD-I (Inclination)	S-A (Anteversion)	CAD-A (Anteversion)
Descriptive (n=140)				
Minimum	15°	15°	1°	1°
Maximum	88°	85°	35°	34°
Mean±SD	50.69±15.56	49.40±15.24	14.36±9.08	14.75±8.58
Normal distribution				
Kolmogorov- Smirnov	p=0.200	p=0.200	p=0.029	p=0.200
Shapiro-Wilk	p=0.513	p=0.670	p=0.001	p=0.001
ICC	0.994		0.992	
F Test with true value 0	p<0.001, 95%CI=0.975-0.997		p<0.001, 95%CI=0.986-0.994	

S-I: Software-measured inclination; CAD-I: CAD-measured inclination; S-A: software-measured anteversion; CAD-A: CAD-measured anteversion; SD: standard deviation; ICC: intraclass correlation coefficient; CI: confidence interval; n: number of measurements.

rejected with the Shapiro-Wilk test (CAD-A: KS $p=0.200$, SW $p=0.001$) (Table I).

The interrater reliability, measured with the intraclass correlation coefficient (ICC), was very high for the inclination measurements (ICC=0.994; 95% CI=0.975-0.997, $p<0.001$). The anteversion measurements also showed a strong correlation between the two methods (ICC=0.992; 95% CI=0.988-0.994, $p<0.001$) (Table I). The measurements were analyzed using a two-way random effects model that considered systematic errors (consistency).

To further evaluate the precision of the software and CAD measurement methods, we conducted an analysis according to the ASTM E691 standard for interlaboratory testing. This standard provides statistical procedures to determine the repeatability and reproducibility of measurement methods. In our context, the two methods (software and CAD) were treated as two different laboratories. The results of the ASTM E691 analysis are summarized in Table II.

For inclination measurements, the repeatability standard deviation (s_r) was 1.39° and the repeatability limit (r) was 3.90°. The between-laboratory standard deviation

Table II. ASTM E691 precision analysis of software versus CAD-based measurement methods.

	Inclination	Anteversion
n	140	140
Repeatability (s_r)	1.39	1.14
Repeatability (r)	3.90	3.18
Between (s_L)	1.07	0.26
Reproducibility (s_R)	1.75	1.17
Reproducibility (R)	4.91	3.27
Bias	1.51	-0.37

(s_L) was 1.07°, resulting in a reproducibility standard deviation (s_R) of 1.75° and a reproducibility limit (R) of 4.91°. The bias between the software and CAD methods was 1.51°. For anteversion measurements, the repeatability standard deviation (s_r) was 1.14° and the repeatability limit (r) was 3.18°. The between-laboratory standard deviation (s_L) was 0.26°, leading to a reproducibility standard deviation (s_R) of 1.17° and a reproducibility limit (R) of 3.27°. The bias was -0.37°.

The small values of s_r and s_R indicate high repeatability and reproducibility for both measurement methods. The repeatability limits (r) of 3.90° for inclination and 3.18° for anteversion are relatively high but clinically within an acceptable range, as they fall within the typical tolerances for acetabular cup positioning (6). The low between-laboratory standard deviation (s_L) for anteversion (0.26°) suggests that the two methods exhibit very similar variability for this parameter, while the slightly higher s_L for inclination (1.07°) indicates somewhat greater disparity between the methods, which is also reflected in the bias.

Discussion

The precise positioning of the acetabular cup is crucial in total hip arthroplasty, as it directly influences patient outcomes, implant longevity, and revision surgery rates (4-6). Inadequate positioning of the hip implant leads to a range of complications, including pain, impingement, implant instability, increased wear, reduced range of motion, and especially dislocations, which often require revision surgery (18, 25, 26). The Lewinnek safety zone, which defines

optimal cup positioning at 40° ($\pm 10^\circ$) inclination and 15° ($\pm 10^\circ$) anteversion, remains a fundamental clinical benchmark in hip arthroplasty (6). Callanan *et al.* (27) at least confirmed Lewinnek *et al.*'s (6) safety zone for inclination, while Dorr *et al.* (28) described these guidelines with the title "Death of the Lewinnek Safe Zone" (27, 28).

Overall, it can be said that anatomical landmarks are still critically discussed today and are dependent on both interobserver variability and patient-specific variability (4-6, 28). Computer-assisted methods enable the assessment of cup positioning with high accuracy within these established parameters without relying on the manual drawing of reference lines on anatomical landmarks, eliminating a potential source of measurement variability.

The high ICC values (>0.99) between the demonstrated software and CAD measurements show that this approach can accurately determine the orientation of the acetabular cup without compromising precision. This is of particular importance in clinical practice, as accurate cup positioning is crucial for optimal function and longevity of the hip joint. The Bland-Altman plot visually supports the high intraclass correlation coefficients and demonstrates the statistical equivalence of computer-assisted and traditional CAD measurement techniques.

The software in this study offers several advantages compared to intraoperative fluoroscopy, CT navigation, and robotic solutions. Intraoperative fluoroscopy solutions such as Radlink and OrthoGrid, which overlay the correct cup position with a template to indicate the optimal end position, have reported successful implantation within the target range for inclination values of 98.2% for Radlink and 97.4% for OrthoGrid ($p=0.384$) (29, 30). Although Radlink is somewhat more time-consuming, Thorne *et al.* recommended its use due to better performance in placement for anteversion (30). For anteversion, Radlink achieved 97.7% of the target range. However, the disadvantage of these solutions is that they rely on their own hardware platforms on image intensifiers and GPS towers, which wirelessly capture images from any X-ray machine (29, 30). The hardware components are associated with corresponding acquisition costs (29, 30). While the intraoperative benefit is undeniable, these

solutions cannot simultaneously evaluate intraoperative X-rays of an acetabular cup and postoperative controls or postoperative X-rays for revision due to misimplantation, as they are hardware-dependent (29, 30).

In contrast, the tested software was designed as a standalone application that does not require specialized hardware beyond a standard computer. With an appropriate server interface to the "Picture Archiving and Communication System" (PACS) and the computer (PC) in the operating room (OR), real-time use would be possible. Application-based smartphone support is planned and could enable real-time analysis through the built-in camera. Furthermore, mathematical angle measurement is possible on various image types. At present, correction assistance or correction suggestions for inadequate implantation are not yet possible but are planned for further studies. The only current support is the ability to verify whether the correct anteversion and inclination have been achieved.

Another way to ensure both preoperative planning and intraoperative support is computer tomography-guided (CT) navigation or computer-assisted surgery (CAS) (31, 32). The preoperative planning of the component position is carried out using CT scans of the patient's pelvis. Intraoperatively, optoelectronic markers are then attached to the pelvic bone as a reference base (13). First, a standardized protocol must be followed, with the surgeon registering landmarks to match the CT scan-based model with the real pelvis (13). The dynamic reference base can then track the position of the pelvis during the procedure (31). The reamer is equipped with an optoelectronic dynamic reference base, allowing the software to visualize the position of the reamer in relation to the pelvis and provide real-time feedback to the surgeon about his movements (31, 32).

It should be noted that a preoperative CT scan is mandatory for these navigation systems, which is associated with corresponding radiation exposure (13). Furthermore, this instrument is linked to a necessary system and cannot provide postoperative control or preoperative planning or measurements for already externally operated patients who are candidates for revision surgery (31). Beyond its application in preoperative planning and intraoperative

positioning control, the software developed in this study also enables the measurement of previously implanted cups based on X-ray imaging, potentially obviating the need for additional CT scans. Whether consistency exists between our measurement approach and the CT-measured anteversion and inclination values needs to be verified in a future study. If this is the case, preoperative planning CT scans for standard cases could become obsolete.

Robot-assisted THA implantation is also based on preoperatively calibrated CT scans (13). From the scan, a three-dimensional model is created, which is used intraoperatively to identify the position of the pelvis based on surface images (33). One of the first robotic systems used in THA was the ROBODOC (THINK Surgical, Fremont, CA, USA) (13). The fully automated arm of the system can prepare the femoral side without the surgeon's intervention (13). However, the system was not used for positioning the acetabular cup component. Currently, the robot arm-assisted surgical technique with a semi-automated robotic system is most commonly used (Mako® THA System, Stryker, Kalamazoo, MI, USA) (33). Here again, optoelectronic antennas with a tracker must be attached and localized to determine the current position (32). A robot arm is positioned during reaming and insertion of the components in relation to the pelvis (33). The system controls and adapts in real-time to the surgeon's hand (33). If the surgeon deviates too far from the preoperative plan, the robot arm resists and warns (33).

While robot-assisted THAs have shown an improvement in the accuracy of component positioning, they, like the CT-guided option, are associated with additional radiation exposure from preoperative CT imaging and represent purely intraoperative support systems (13). In contrast, the presented software only requires standard X-ray images, reducing radiation exposure while still enabling accurate measurements.

Despite the promising results, several methodological limitations in the current implementation warrant consideration prior to clinical application. Foremost, the tested approach has thus far been validated exclusively on a single phantom with one implant type under controlled radiographic conditions. Patient anatomy

exhibits considerable heterogeneity, necessitating evaluation of our algorithm's performance across diverse patient populations with varying body habitus, pelvic orientations, and implant designs.

Secondly, our study employs a phantom-to-X-ray-to-measurement approach, which may introduce potential errors during the radiographic acquisition phase. Alternative validation methodologies exist, such as the direct synthesis of radiographic images using computational approaches like the THR Simulator developed by Wu *et al.* (34), which can generate synthetic radiographs with predefined parameters and eliminate acquisition-related variabilities. However, our use of a physical phantom was chosen specifically to replicate realistic clinical imaging conditions, incorporating actual radiographic artifacts and variations while ensuring mechanical consistency in cup positioning. Future work could beneficially combine both approaches, using synthetic radiographs for initial algorithm development and physical phantoms for clinical validation. The current implementation necessitates partial manual intervention, requiring users to either place points along the cup rim or define cup axes. A fully automated system would be preferable to minimize inter-observer variability and reduce measurement time. It is important to note that our preliminary automated detection achieving an 80% detection rate on phantom images was accomplished using the RANSAC mathematical fitting algorithm rather than artificial intelligence methods. Furthermore, no computer vision framework integration has yet been implemented. While these results are encouraging, substantial improvement and validation in clinical settings remain essential prerequisites.

Additionally, previous validation efforts have not yet incorporated comparisons with three-dimensional computed tomography measurements, which are regarded as superior to two-dimensional radiographic measurements for determining actual cup orientation. This validation will be indispensable for confirming the accuracy of our approach within a three-dimensional context in subsequent investigations. Finally, our software currently functions as a standalone application without integration

into hospital PACS or intraoperative imaging devices. Such integration represents a necessary prerequisite for seamless clinical implementation.

Conclusion

Future research endeavors should prioritize several key aspects: refinement of automatic detection algorithms, comprehensive validation across diverse patient demographics, development of seamless integration protocols for hospital imaging ecosystems, and execution of comparative analyses with three-dimensional imaging modalities.

In summary, our investigation has yielded the development and validation of a computer-assisted measurement technique for acetabular cup positioning assessment, demonstrating exceptional concordance with current standard methodologies while conferring significant workflow advantages. The encouraging results obtained provide a robust foundation upon which implementation within established computer vision models can be constructed, ultimately enabling automated three-dimensional spatial positioning recognition of the acetabular cup. This approach represents a promising advancement toward more accessible, accurate, and efficient cup position measurement that could be seamlessly integrated throughout the entire care continuum from preoperative planning to postoperative evaluation. Subsequent development initiatives will concentrate on enhancing automation through established CV frameworks, validating applicability across heterogeneous patient populations and implant designs, and conducting comparative analyses with three-dimensional computed tomography measurements to ensure comprehensive clinical utility.

Conflicts of Interest

The Authors declare no conflicts of interest.

Authors' Contributions

G.A., S.S., T.OP. S.D. and E.L. conceptualized and designed the study; L.H. created the executable software, and S.D. and P.H.

revised and finalized the final version; G.A. T.OP. L.H. and S.D. evaluated and interpreted the data; G.A. and T.OP., J.C., and J.M. collected the data; G.A. and T.OP. led the study and drafted the study manuscript and S.S., E.L., S.D and P.H. substantively revised the manuscript. All the Authors contributed to the manuscript and agreed with its submission.

Artificial Intelligence (AI) Disclosure

The Authors utilized artificial intelligence tools (Claude 4, Anthropic, accessed May 26, 2025) for assistance with medical writing, grammar, language editing, and reporting standards. All scientific content, methodology, data interpretation, and conclusions remain entirely the intellectual work of the authors. The Authors take full responsibility for the integrity, accuracy, and correctness of all aspects of this work, including any content that received AI assistance for language and formatting purposes.

References

- 1 Learmonth ID, Young C, Rorabeck C: The operation of the century: total hip replacement. *Lancet* 370(9597): 1508-1519, 2007. DOI: 10.1016/S0140-6736(07)60457-7
- 2 Charnley J: Arthroplasty of the hip: a new operation. *Lancet* 277(7187): 1129-1132, 1961. DOI: 10.1016/S0140-6736(61)92063-3
- 3 Patel I, Nham F, Zalikha L, El-Othmani MM: Epidemiology of total hip arthroplasty: demographics, comorbidities and outcomes. *Arthroplasty* 5(1): 2, 2023. DOI: 10.1186/s42836-022-00156-1
- 4 Enge Júnior DJ, Castro ADAE, Fonseca EKUN, Baptista E, Padiál MB, Rosemberg LA: Main complications of hip arthroplasty: pictorial essay. *Radiol Bras* 53(1): 56-62, 2020. DOI: 10.1590/0100-3984.2018.0075
- 5 Goe TJ: Dislocation following revision total hip arthroplasty. *Am J Orthop (Belle Mead, NJ)* 31(4): 225-227, 2002.
- 6 Lewinnek GE, Lewis JL, Tarr R, Compere CL, Zimmerman JR: Dislocations after total hip-replacement arthroplasties. *J Bone Joint Surg Am* 60(2): 217-220, 1978.
- 7 Philippot R, Adam P, Reckhaus M, Delangle F, Verdote FX, Curvale G, Farizon F: Prevention of dislocation in total hip revision surgery using a dual mobility design. *Orthop Traumatol Surg Res* 95(6): 407-413, 2009. DOI: 10.1016/j.otsr.2009.04.016
- 8 Sharma AK, Vigdorichik JM: The hip-spine relationship in total hip arthroplasty: how to execute the plan. *J Arthroplasty* 36(7): S111-S120, 2021. DOI: 10.1016/j.arth.2021.01.008

- 9 Loitsch T, Freitag T, Leucht F, Reichel H, Bieger R: [Measurement of acetabular cup inclination in anteroposterior pelvic radiogram: An indicator of quality after primary total hip arthroplasty?]. *Orthopade* 47(12): 1003-1008, 2018. DOI: 10.1007/s00132-018-3628-2
- 10 Zhao JX, Su XY, Zhao Z, Xiao RX, Zhang LC, Tang PF: Radiographic assessment of the cup orientation after total hip arthroplasty: a literature review. *Ann Transl Med* 8(4): 130, 2020. DOI: 10.21037/atm.2019.12.150
- 11 McLaren RH: Prosthetic hip angulation. *Radiology* 107(3): 705-706, 1973. DOI: 10.1148/107.3.705
- 12 Vigdorichik JM, Muir JM, Buckland A, Elbuluk AM, Alguire A, Schipper J, Schwarzkopf R: Undetected intraoperative pelvic movement can lead to inaccurate acetabular cup component placement during total hip arthroplasty: a mathematical simulation estimating change in cup position. *J Hip Surg* 01(04): 186-193, 2017. DOI: 10.1055/s-0038-1635103
- 13 Sai Sathikumar A, Jacob G, Thomas AB, Varghese J, Menon V: Acetabular cup positioning in primary routine total hip arthroplasty-a review of current concepts and technologies. *Arthroplasty* 5(1): 59, 2023. DOI: 10.1186/s42836-023-00213-3
- 14 Fukunishi S, Fukui T, Imamura F, Nishio S, Shibamura N, Yoshiya S: Assessment of accuracy of acetabular cup orientation in CT-free navigated total hip arthroplasty. *Orthopedics* 31(10): e1-e4, 2008. DOI: 10.3928/01477447-20110525-13
- 15 Tetsunaga T, Yamada K, Tetsunaga T, Furumatsu T, Sanki T, Kawamura Y: Comparison of the accuracy of CT- and accelerometer-based navigation systems for cup orientation in total hip arthroplasty. *Hip Int* 31(5): 603-608, 2021. DOI: 10.1177/1120700020904940
- 16 Ando W, Takao M, Hamada H, Uemura K, Sugano N: Comparison of the accuracy of the cup position and orientation in total hip arthroplasty for osteoarthritis secondary to developmental dysplasia of the hip between the Mako robotic arm-assisted system and computed tomography-based navigation. *Int Orthop* 45(7): 1719-1725, 2021. DOI: 10.1007/s00264-021-05015-3
- 17 Takada R, Jinno T, Miyatake K, Hirao M, Yoshii T, Okawa A: Portable imageless navigation system and surgeon's estimate for accurate evaluation of acetabular cup orientation during total hip arthroplasty in supine position. *Eur J Orthop Surg Traumatol* 30(4): 707-712, 2020. DOI: 10.1007/s00590-020-02625-2
- 18 Patel N, Golwala P: Approaches for total hip arthroplasty: a systematic review. *Cureus* 15(2): e34829, 2023. DOI: 10.7759/cureus.34829
- 19 Obermeyer Z, Emanuel EJ: Predicting the future - big data, machine learning, and clinical medicine. *N Engl J Med* 375(13): 1216-1219, 2016. DOI: 10.1056/NEJMp1606181
- 20 Long X, Deng K, Wang G, Zhang Y, Dang Q, Gao Y, Shen H, Ren J, Han S, Ding E, Wen S: PP-YOLO: An effective and efficient implementation of object detector. *arXiv: 2007.12099*, 2020. DOI: 10.48550/arXiv.2007.12099
- 21 Lavanya G, Pande SD: Enhancing real-time object detection with YOLO algorithm. *EAI Endorsed Trans IoT* 10, 2024. DOI: 10.4108/eetiot.4541
- 22 Ramachandran S, George J, Skaria S, V.v. V: Using YOLO based deep learning network for real time detection and localization of lung nodules from low dose CT scans. *Proc SPIE*: 53, 2018. DOI: 10.1117/12.2293699
- 23 Liodakis E, Pöhler GH, Sonnow L, Mommsen P, Clausen JD, Gaulich T, Maslaris A, Omar M, Stübig T, Sehmisch S, Omar Pacha T: Validation of direct CT measurement of malrotation in femoral neck fractures: A bone model study. *PLoS One* 18(4): e0278850, 2023. DOI: 10.1371/journal.pone.0278850
- 24 Fleiss JL: *The design and analysis of clinical experiments*. New York, NY, USA, John Wiley & Sons, Inc., 1999. DOI: 10.1002/9781118032923
- 25 Fujishiro T, Hiranaka T, Hashimoto S, Hayashi S, Kurosaka M, Kanno T, Masuda T: The effect of acetabular and femoral component version on dislocation in primary total hip arthroplasty. *Int Orthop* 40(4): 697-702, 2016. DOI: 10.1007/s00264-015-2924-2
- 26 Siebenmorgen JP, Stronach BM, Mears SC, Stambough JB: The use of intraoperative digital radiography alignment software to assess implant placement in total hip arthroplasty. *Curr Rev Musculoskelet Med* 14(6): 369-377, 2021. DOI: 10.1007/s12178-021-09722-7
- 27 Callanan MC, Jarrett B, Bragdon CR, Zurakowski D, Rubash HE, Freiberg AA, Malchau H: The John Charnley Award: risk factors for cup malpositioning: quality improvement through a joint registry at a tertiary hospital. *Clin Orthop Relat Res* 469(2): 319-329, 2011. DOI: 10.1007/s11999-010-1487-1
- 28 Dorr LD, Callaghan JJ: Death of the Lewinnek "Safe Zone". *J Arthroplasty* 34(1): 1-2, 2019. DOI: 10.1016/j.arth.2018.10.035
- 29 Debbi EM, Rajae SS, Mayeda BF, Penenberg BL: Determining and achieving target limb length and offset in total hip arthroplasty using intraoperative digital radiography. *J Arthroplasty* 35(3): 779-785, 2020. DOI: 10.1016/j.arth.2019.10.003
- 30 Thorne T, Nishioka S, Andrews S, Mathews K, Nakasone C: Component placement accuracy of two digital intraoperative fluoroscopy supplementation systems in direct anterior total hip arthroplasty. *Arch Orthop Trauma Surg* 142(6): 1283-1288, 2022. DOI: 10.1007/s00402-021-04008-6
- 31 Kelley TC, Swank ML: Role of navigation in total hip arthroplasty. *J Bone Joint Surg Am* 91(Supplement 1): 153-158, 2009. DOI: 10.2106/JBJS.H.01463
- 32 Stübig T, Windhagen H, Krettek C, Ettinger M: Computer-assisted orthopedic and trauma surgery. *Dtsch Arztebl Int* 117(47): 793-800, 2020. DOI: 10.3238/arztebl.2020.0793
- 33 Kayani B, Konan S, Ayuob A, Ayyad S, Haddad FS: The current role of robotics in total hip arthroplasty. *EFORT Open Rev* 4(11): 618-625, 2019. DOI: 10.1302/2058-5241.4.180088
- 34 Wu TY, Yang RS, Fuh CS, Hou SM, Liaw CK: THR Simulator--the software for generating radiographs of THR prosthesis. *BMC Musculoskelet Disord* 10: 8, 2009. DOI: 10.1186/1471-2474-10-8